



## ORIGINAL ARTICLE

# Preparation and evaluation of physicochemical properties and anti-leishmanial activity of zirconium/tioxolone niosomes against *Leishmania major*



Parisa Fatehi chinar<sup>a</sup>, Sina Bahraminejad<sup>b,c,\*</sup>, Abbas Pardakhty<sup>c</sup>, Iraj Sharifi<sup>b</sup>, Mahdi Ranjbar<sup>c,d,\*</sup>, Somayyeh Karami-Mohajeri<sup>c</sup>, Fatemeh Sharifi<sup>b</sup>

<sup>a</sup> Neuroscience Research Center, Institute of Neuropharmacology, Kerman University of Medical Sciences, Kerman, Iran

<sup>b</sup> Leishmaniasis Research Center, Kerman University of Medical Sciences, Kerman, Iran

<sup>c</sup> Pharmaceutics Research Center, Institute of Neuropharmacology, Kerman University of Medical Sciences, Kerman, Iran

<sup>d</sup> Health in Disasters and Emergencies Research Center, Institute for Futures Studies in Health, Kerman University of Medical Sciences, Kerman, Iran

Received 7 May 2022; accepted 25 July 2022

Available online 29 July 2022

## KEYWORDS

Niosome;  
Drug delivery;  
Anti-leishmanial effects;  
*Leishmania major*

**Abstract** Due to the limitations of current chemotherapy for the treatment of leishmaniasis, there is an urgent requirement to search for new anti-leishmanial compounds and nano-drug delivery systems including niosomes. Therefore, the aim of this study was to prepare zirconium/tioxolone niosomes using the film hydration method and evaluate the physicochemical properties of the produced niosomes including morphology, size distribution, stability, and encapsulation efficiency. The best formulation was chosen as Span/Tween 40 (N<sub>ZT1</sub>) due to its physicochemical properties, and leishmanicidal activity against promastigotes and amastigotes was measured using both 3-(4,5-dimethyl thiazol2yl)-2,5-diphenyltetrazolium bromide (MTT) and flow cytometry methods. In addition, to assess the mechanism of action of the prepared niosomes, apoptosis, levels of gene expression, reactive oxygen species (ROS) generation, superoxide dismutase (SOD) activity, and nitrite production were evaluated. The prepared formulation indicated log-normal particle size distribution curves, high encapsulation efficiency (more than 95.72 %), and good physical stability after one week, three months, and six months. Our findings demonstrated that amphotericin B was more effective than

\* Corresponding authors at: Pharmaceutics Research Center, Institute of Neuropharmacology, Kerman University of Medical Sciences, Kerman, Iran.

E-mail addresses: [S.bahraminejad@kmu.ac.ir](mailto:S.bahraminejad@kmu.ac.ir) (S. Bahraminejad), [Mehdi.Ranjbar@kmu.ac.ir](mailto:Mehdi.Ranjbar@kmu.ac.ir) (M. Ranjbar).

Peer review under responsibility of King Saud University.



Zr/tioxolone niosomes (NZTs) due to the selectivity index (SI). However, the niosomal formulation of Zr/tioxolone showed no cytotoxic effect within the range of our experimental concentrations (CC<sub>50</sub> of 308.21 µg/mL). Moreover, the prepared niosomes increased the expression level of interleukin (IL)-12 and inducible nitric oxide synthase (iNOS) and significantly decreased the expression level of the IL-10 gene, which confirms the immunomodulatory role of NZTs. According to our findings in this study, the niosomal form of this combination can be considered for further therapeutic approaches against *L. major* in future planning.

© 2022 The Author(s). Published by Elsevier B.V. on behalf of King Saud University. This is an open access article under the CC BY-NC-ND license (<http://creativecommons.org/licenses/by-nc-nd/4.0/>).

## 1. Introduction

Leishmaniasis is a group of tropical diseases caused by intracellular protozoan parasites of the genus *Leishmania* from the *Trypanosomatidae* family. Female phlebotomine sandflies transmit it between mammalian hosts (W.H. Organization, 2017). The World Health Organization (WHO) ranked leishmaniasis next to malaria as the most lethal protozoan disease (Kumari et al., 2021). Its clinical features range from small skin ulcers in cutaneous leishmaniasis (CL) to serious systemic manifestations in visceral leishmaniasis (VL). Leishmaniasis is a widespread disease in more than 90 countries belonging to Asia, Africa, America, and Europe (Steveding, 2017). Afghanistan, Saudi Arabia, Algeria, Brazil, Iran, Iraq, Syria, and Sudan are countries where more than 90 % of the cases of CL have been reported (Monzote, 2009). According to the WHO, about 0.6–1.0 million new cases of CL and 0.2–0.4 million new cases of VL have recorded annually around the world (Singh et al., 2016). *Leishmania major* and *L. tropica* are the two *Leishmania* species that cause CL in the old world (Bahraminegad et al., 2021; Akbari et al., 2017). Several limitations including high toxicity, numerous adverse effects, the appearance and prevalence of resistant strains, length of treatment, and the high cost of current chemotherapy, which includes pentavalent antimonials, amphotericin B, pentamidine, miltefosine, and aminosidine, are the main concerns in the leishmaniasis epidemic (Bahraminegad et al., 2021; Singh and Sivakumar, 2004). Therefore, there is an urgent requirement to search for new anti-leishmanial compounds. Designing nano-drug delivery systems for conventional drugs and nanonization of drugs are two approaches of nanotechnology in the treatment of this infection (Müller et al., 2001; Vyas and Gupta, 2006). These drug delivery systems result in pharmacokinetic properties, high efficacy, high target delivery effect, low toxicity, high concentration, releasing drugs with a controlled system, and prolonged systemic circulation lifetime (de Carvalho et al., 2013). According to numerous investigations, niosomes (non-ionic surfactant vesicles) are one of the best drug delivery systems among these carriers due to the presence of hydrophilic, amphiphilic, and lipophilic moieties in their structure, which can incorporate drug molecules with a broad range of solubility (Kazi et al., 2010; Jain, 1997). Biodegradable, biocompatible, and non-immunogenic surfactants should be used to synthesize niosomes (Hu and Rhodes, 1999). Although the *in vivo* behavior of niosomes is similar to liposomes, some advantages such as better drug entrapment efficiency, lower prices, and the higher chemical stability of their ingredients make niosomes a better choice (Kazi et al., 2010). One of the benefits of using this drug delivery system in the treatment of leishmaniasis is that the reticuloendothelial system takes up the niosomal vesicles and accumulates them there. Thus, this vesicular system provides better concentration of the drug administered by topical path at the site of action, which helps localize the drug at the site of administration (Baillie et al., 1986; Hunter et al., 1988). Table 1 demonstrated some of the recent researches for application of niosomes treatment of leishmaniasis.

Zirconia (ZrO<sub>2</sub>) is one of the widely used metal oxide nanoparticles for potential bio-applications such as tissue regeneration and cancer therapy due to its high mechanical strength, low toxicity, and superior biocompatibility. Similar to other metal nanoparticles, reactive oxygen

species (ROS) play a vital role in the ZrO<sub>2</sub> nanoparticle-induced cytotoxicity, including changes in cell viability, apoptosis, and necrosis, which cause microbial damage (Bahraminegad et al., 2021; Ye and Shi, 2018; Patil and Kandasubramanian, 2020). Tioxolone (C<sub>7</sub>H<sub>4</sub>O<sub>3</sub>S), which is known as an anti-fungal, anti-bacterial, anti-inflammatory, and anti-tumorigenic compound, has been proven to be effective for the local treatment of acne and psoriasis vulgaris (Parizi et al., 2019). Thus, we carried out this *in vitro* study using various concentrations of zirconium combined with tioxolone in its niosomal formulation to investigate their anti-leishmanial effects on *L. major* via both 3-(4,5-dimethylthiazol-2-yl)-2,5-diphenyltetrazolium bromide (MTT) and flow cytometry methods.

## 2. Materials and methods

### 2.1. Materials

All reagents were used without further purification and were of analytical grade. Fetal calf serum (FCS) and RPMI-1640 medium containing L-glutamine were procured from Gibco (Eching, Germany), and the MTT powder and amphotericin B as the control drug were purchased from Sigma-Aldrich (St Louis, MO). Penicillin and streptomycin were obtained from Alborz Pharmacy (Karaj, Iran) and were stored at room temperature (25 °C) until the experiments.

### 2.2. Cell line and parasite strains

Promastigotes of the standard strain of *L. major* (MRHO/IR/75/ER) were acquired from the Leishmaniasis Research Center (Kerman, Iran) and cultured in Novy-MacNeal-Nicolle (NNN) medium. Then they were incubated at 24 °C ± 1 and subcultured into RPMI-1640 medium supplemented with 10 % heated fetal bovine serum (HFBS) and 1 % penicillin/streptomycin (Pen/Strep) antibiotics. After that, they were incubated at 25 °C where they slowly differentiated into metacyclic forms for the next usage. Murine macrophage cells J774 A.1 ATCC®TIB-67™ were purchased from the Pasteur Institute of Iran. The J744 cell line was placed in a flask and cultured in Dulbecco's modified eagle medium (DMEM) enriched with 10 % HFBS and 1 % Pen/Strep antibiotics and maintained at 37 °C in 5 % CO<sub>2</sub>.

### 2.3. Preparation of Zr/tioxolone niosomes (NZTs)

Initially, in order to prepare a solution containing the zirconium salt, 0.01 g of Zr(NO<sub>3</sub>)<sub>4</sub>, 0.02 g of sodium dodecyl sulfate (CTAB), and 10 mL of sodium hydroxide (2 M) were dissolved under a reflux system for 30 min and stirred at a speed of 400 rpm using a magnetic stirrer. Then, after adding 5 mL of

**Table 1** Some of the recent researches for application of niosomes treatment of leishmaniasis.

Niosomal combinations	Method	Leishmania species	Stage employed	Reference
Selenium with glucantime	Film hydration	<i>L. tropica</i>	PromastigoteAmastigote	(Mostafavi et al., 2019)
Benzoxonium chloride	Film hydration	<i>L. tropica</i>	PromastigoteAmastigote	(Parizi et al., 2019)
Autoclaved <i>Leishmania major</i>	Film hydration	<i>L. major</i>	BALB/c mice	(Pardakhty et al., 2012)
Amarogentin	Film hydration	<i>L. donovini</i>	Hamster	(Medda et al., 1999)
Sodium stibogluconate mixed with paramomycin	Film hydration	<i>L. infantum</i>	Beagle dog	(Miret et al., 2021)

N, *N*-dimethylformamide (DMF), 4 mL of double-distilled water was added to the reaction medium. Afterward, the mixture was placed in a microwave oven at a power of 180 W for 15 min. Niosomal vesicles were prepared using the film hydration method (Mohammadi et al., 2016; Bucks et al., 2009). Briefly, the lipid phase containing the nonionic surfactants (Span/Tween 20, 40, 60, and 80) and cholesterol were dissolved in chloroform and mixed at a 7/3 M ratio, and the organic solvent was omitted using a rotary evaporator (Büchi Labortechnik AG, Switzerland) at 65 °C for 30 min. After that, the hydration of the obtained film was performed by 5 mL of deionized water, in which tioxelone solution (0.2 % w/v in phosphate-buffered saline (PBS), pH 6.8) was dissolved at 65 °C for 30 min. The resulting niosomal suspensions were maintained overnight at the refrigerator temperature. Then, the prepared zirconium solution was added dropwise to the niosomes containing the tioxelone mixture with a ratio of 1:1 under a reflux system at 40 °C for 30 min and stirred at a speed of 300 rpm using a magnetic stirrer. Finally, the resulting mixture was placed in a microwave at 100 W for 3 min. Samples were stored in glass vials for six months and were withdrawn at regular time intervals (one week and three and six months).

#### 2.4. Characterization of prepared niosomes

Light microscopy (Zeiss, Oberkochen, Germany) was used to evaluate the morphology of the niosomal formulations using the camera that was attached to it, equipped with a computer-controlled image analysis system. Dynamic light scattering was employed to assess the size dispersion of the niosomes via measuring the hydrodynamic diameter by the Malvern apparatus (Malvern Mastersizer X, Malvern, UK), and niosomal size was determined as a physical stability indicator. The encapsulation efficiency was evaluated using a UV-visible spectrophotometer at 287.9 nm. For this purpose, 1 mL of isopropyl alcohol was added to the pellet to dissolve the walls of the niosomes and the amount of the entrapped drug was calculated using the following equation:

$$\% \text{ Encapsulation efficiency} = \frac{[(\text{Total drug} - \text{free non-entrapped}) / \text{Total drug}] \times 100}{(1)}$$

#### 2.5. Evaluation of the antioxidant effect

The hydrogen donation ability of the prepared niosomes was assessed using a spectrophotometric assay that employs stable 2,20-diphenyl-1-picrylhydrazyl (DPPH) radical as a reagent.

For this purpose, the scavenging activity of DPPH was evaluated by bleaching the purple-colored methanol solution. Briefly, 1 mL of different concentrations of NZTs (1–1000 µg/mL) was added to 1 mL of freshly prepared DPPH solution in methanol (0.15 mM) and then 3 mL of methanol was added to the reaction mixture. After that, the sample was kept in the dark for 30 min, and its absorbance was read at 517 nm. This procedure was repeated for butylated hydroxyanisole (BHA) as the positive control, which is a synthetic antioxidant, and deionized water was used as the control. Tests were carried out in triplicate. The inhibition percentage of DPPH was calculated using the following equation:

$$\text{Inhibition percentage of DPPH (\%)} = [1 - (A_a - A_b) / A_c] \times 100 \quad (2)$$

where  $A_a$  is the absorbance of the samples mixed with DPPH solution,  $A_b$  is the absorbance of the samples without DPPH solution, and  $A_c$  is the absorbance of the control solution. The sample concentration that causes 50 % inhibition of DPPH ( $IC_{50}$ ) is calculated using a linear regression model.

#### 2.6. Anti-promastigote assay (MTT assay)

To evaluate the in vitro anti-leishmanial activity of zirconium/tioxelone niosomes against the promastigote forms of *Leishmania major*, MTT was used as a marker of cell viability. For this purpose, the RPMI-1640 medium supplemented with 10 % FBS, which contained  $2 \times 10^5$  cells/mL promastigotes in the logarithmic growth phase, was seeded in 96-well flat-bottom plates at 100 µL/well. After that, several concentrations of the niosomal forms of zirconium/tioxelone were added to triplicate wells at 10 µL/well. Meanwhile, a medium with no drugs was used as the negative control and plates were incubated for 72 h at 25 °C. Then, a stock solution of MTT (Sigma Chemical Co., St. Louis, Mo.) was prepared at a concentration of 5 mg/mL by dissolving MTT in PBS and storing it in the dark at 4 °C for up to two weeks before use. At the end of incubation, 10 µL of MTT was added to each well and the plates were incubated for 4 h at 25 °C. Finally, the reaction was terminated by dimethyl sulfoxide (DMSO) and relative optical density (OD) was measured using an ELISA reader at 490 nm.

#### 2.7. Anti-amastigote assay

To carry out the anti-amastigote assay, the stationary phase promastigotes of *L. major* ( $25 \times 10^5$ ) were added to the murine macrophage cell line (J774 A.1 ATCC®TIB-67™) ( $25 \times 10^4$ ) at a ratio of 10:1 (promastigote: macrophage).

After incubation at 37 °C and in 5 % CO<sub>2</sub> for 24 h, the pipetting of fresh RPMI-1640 medium was conducted to wash and remove free parasites. Then intra-macrophage amastigotes were treated with different concentrations of NZTs and the conventional form of amphotericin B as a positive standard drug, and they were incubated again under the same conditions for 72 h. Finally, the treated slides were dried, fixed with methanol, stained by Giemsa, and accurately evaluated under a light microscope (Nikon, Japan). In addition, amastigote-infected macrophages with no drugs and macrophages with no parasites and drugs were considered as untreated and negative groups, respectively. This method was repeated thrice and the IC<sub>50</sub> values were calculated for both drugs using the probit test.

### 2.8. Cytotoxicity assay

The flow cytometry analysis was carried out to investigate the cytotoxicity of J774A.1 ATCC®TIB-67™ and determine the CC<sub>50</sub> (cytotoxicity concentration for 50 % of cells). For this purpose, 1 × 10<sup>6</sup> macrophages were seeded into 1.5-mL microtubes. After adding 100 µL of various concentrations of Zr plus tioxolone niosomes (25 + 25, 50 + 50, and 100 + 100 µg/mL), all samples were incubated at 37 °C in 5 % CO<sub>2</sub> for 72 h. The tubes without any drugs were considered as negative controls. After the samples were washed twice with cold PBS solution, the PE Annexin V Apoptosis Detection Kit I (BD Pharmingen™) was used for the detection of apoptotic and necrotic cells by adding 500 µL of binding buffer, 5 µL of annexin V, and 5 µL of propidium iodide (PI). Finally, all the samples were incubated at room temperature (25 °C) in dark conditions for 20 min and a flow cytometer (BD FACSCalibur, San Jose, California, USA) and flowing software 2 were used to analyze the data. The flow cytometry assay was performed in duplicate.

### 2.9. Flow cytometry assay

For the evaluation of drug cytotoxicity and apoptosis, the PE Annexin V Apoptosis Detection Kit I (BD Pharmingen™) was employed to determine the cellular viability ranges of *L. major* promastigotes exposed to drugs (NZTs and the conventional form of amphotericin B as a positive control). For this purpose, 10<sup>6</sup> exposed promastigotes of *L. major* with 100 µL of different concentrations of drugs were seeded in 1.5-mL microtubes and incubated at 25 °C in a 5 % CO<sub>2</sub> incubator for 72 h using a modified method previously described by Bahraminegad et al. (Bahraminegad et al., 2021). Next, the cells were washed twice with cold PBS and 100 µL of the solution was transferred to a 5-mL culture tube. After that, 5 µL of PE Annexin V and 5 µL of 7-aminoactinomycin D (7-AAD) were added to the resulting mixture and incubated at room temperature (25 °C) in darkness for 20 min. Finally, after adding 400 µL of 1X binding buffer, all samples were analyzed using a flow cytometer (BD FACSCalibur, San Jose, California, USA). In addition, the samples containing only the medium and parasites with no drugs were considered as untreated controls. The flow cytometry assay was carried out in duplicate.

### 2.10. Intracellular ROS generation

In order to determine the level of intracellular ROS in intra-macrophage amastigotes, the redox-sensitive dye, 2,7-dichlorodihydrofluorescein diacetate (H2DCF-DA), was used. For this purpose, the stationary phase promastigotes of *L. major* (25 × 10<sup>5</sup>) were added to the murine macrophage cell line (J774 A.1 ATCC®TIB-67™) (25 × 10<sup>4</sup>) at a ratio of 10:1 (promastigote: macrophage) in 96-well flat-bottom plates. After incubation at 37 °C and in 5 % CO<sub>2</sub> for 24 h, the supernatants were removed and 100 µL of the DMEM medium supplemented with 10 % FBS was added to each well and then the cells were exposed to drugs (NZTs and the conventional form of amphotericin B as a positive control) for 72 h. In the next step, 200 µL of H2DCF-DA (10 mM) was added to each well. After incubation at 37 °C in 5 % CO<sub>2</sub> for 45 min, the cells were washed twice with PBS. Finally, representative images were evaluated and recorded on a fluorescence microscope.

### 2.11. Evaluation of superoxide dismutase (SOD) activity

In order to determine SOD activity in amastigotes, the SOD assay kit (SOD assay kit, Calbiochem) was used based on the manufacturer's protocol. For this purpose, 10<sup>6</sup> promastigotes exposed to 100 µL of different concentrations of NZTs were seeded in 96-well flat-bottom plates. After individual incubation (at 37 °C in 5 % CO<sub>2</sub>) for 72 h, 20 mM cold HEPES buffer (pH-7.2, containing 1 mM EGTA, 210 mM mannitol, and 70 mM sucrose) was used to homogenize the parasites. Finally, after adding 200 µL of diluted radical detector and 20 µL of diluted xanthine oxidase to 10 µL of the collected supernatants, parasites were incubated for 20 min. OD was then measured using an ELISA reader at 420 nm. This assay was performed in triplicate and data were expressed as mean ± standard deviation (SD).

### 2.12. Nitrite assay

In this spectrophotometric assay, after exposing axenic amastigotes to different concentrations of NZTs, they were incubated at 37 °C in 5 % CO<sub>2</sub> for 72 h and the supernatants were collected. Next, nitrite, a by-product of nitric oxide (NO), was measured by adding the Griess reagent (0.1 % N-1-naphthylethylenediamine in 5 % phosphoric acid and 1 % sulfanilamide) to the same volume of supernatants. Finally, after 10–15 min of incubation at room temperature, measurements were carried out at 540 nm. This assay was performed in triplicate and data were expressed as mean ± SD.

### 2.13. Gene expression, RNA extraction, and cDNA synthesis

The RNeasy Mini Kit (Qiagen, Chatsworth, California, USA) was used to extract total RNA from intra-murine macrophage amastigotes treated with various concentrations of NZTs and untreated control groups based on the manufacturer's protocol. A Nanodrop spectrophotometer (ND-2000, Thermo Scientific Fisher, US) was employed to evaluate the quantity

(ng) and purity of the extracted RNA. The RT reagent kit (Takara, Japan) was used to synthesize cDNA. Quantitative real-time polymerase chain reaction (qPCR) assay was carried out to detect relative expression levels of interleukin (IL)-12 p40, inducible nitric oxide synthase (iNOS), and IL-10 in murine macrophage cells (J774 A.1). The qPCR reaction was executed in duplicate using the Rotorgene Cyclor system (Rotor-Gene Q, Corbett, Qiagen) and a SYBR Green experiment (SYBR Premix Ex Taq™ II, Takara Bio, Inc., Shiga, Japan) based on the recommended protocol. Specific primers and glyceraldehyde 3-phosphate dehydrogenase (GAPDH) as a reference gene are shown in Table 2 [28–30]. The qPCR steps were as follows: 40 three-step cycles (10 s at 95 °C for denaturation of DNA, 15 s at 58 °C for primer annealing, and 20 s at 72 °C for extension) were completed for cDNA amplification after the temperature was kept at 95 °C for 1 min. Finally, qPCR was finished by setting the temperature at 65 °C for 1 min. Gene expression level was specified by the  $2^{-\Delta Ct}$  method (Sharifi et al., 2021; Mostafavi et al., 2019).  $\Delta Ct$  was calculated using the following equation:

$$\Delta Ct = Ct(\text{target}) - Ct(\text{reference}) \quad (3)$$

#### 2.14. Statistical analyses

Prism 7.01 software (GraphPad Software, CA, USA) was used to carry out statistical data analyses using one-way analysis of variance (ANOVA) and Tukey's post-hoc test to evaluate the differences between the treatment groups. GRAPHPAD PRISM 6 (Graph Pad Software Inc, San Diego, CA, USA) was employed to compare and analyze the mean  $2^{-\Delta Ct}$  for the treatment group and the mean  $2^{-\Delta Ct}$  for the control group for each cytokine. The  $IC_{50}$  and  $CC_{50}$  values were determined by the probit analysis using SPSS software ver. 20 (Chicago, Illinois, USA) and  $P \leq 0.05$  was considered statistically significant.

### 3. Results

#### 3.1. Characterization of prepared niosomes

NZTs were formed as shown in Fig. 1. Span/Tween 40 (NZT<sub>1</sub>) was chosen as the best formulation due to the morphology of the prepared niosomes (round multilamellar vesicles) and their particle size distribution. The prepared formulation exhibited log-normal particle size distribution curves, and as demonstrated in its size distribution curves after one week, three months, and six months, NZT<sub>1</sub> had good physical stability. In addition, high encapsulation efficiency (more than 95.72 %) was obtained for NZT<sub>1</sub> (Table 3).

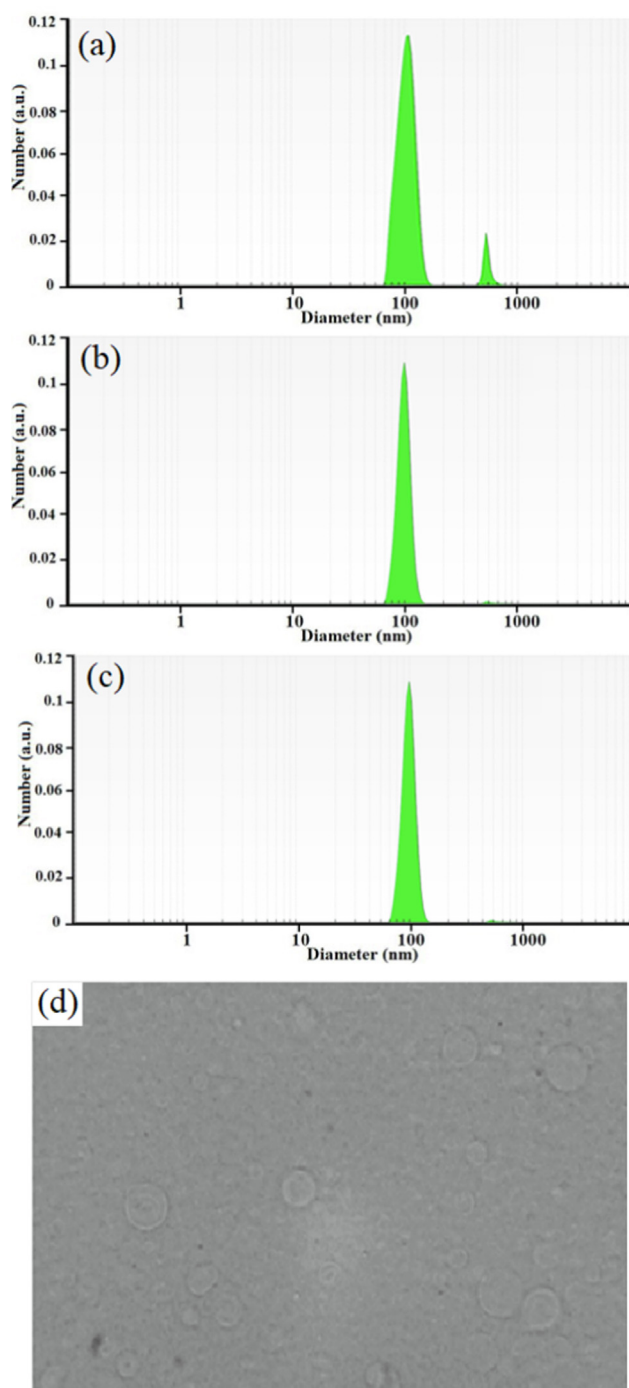


**Fig. 1** The particle size distribution graphs at 1 week (a), 3 (b) and 6 months (c) and the light microscopic picture of niosomal forms of Zr/tioxolone ( $\times 100$  magnification) prepared by film hydration method (d).

**Table 2** The specific primers and genes sequences.

Gene	Forward sequence (5'-3')	Reverse sequence (5'-3')	Product size (bp)
IL-12 P40	CTGGAGCACTCCCATTCTTA	GCAGACATTCCCGCCTTTG	160
IL-10	CTTACTGACTGGCATGAGGATCA	GCAGCTCTAGGAGCATGTGC	101
iNOS	ACATCGACCCGTCCACAGTAT	CAGAGGGGTAGGCTTGTCTC	89
GAPDH	AGCTTCGGCACATATTCATCTG	CGTTCACCTCCCATGACAAACA	89

**Table 3** Encapsulation efficiency percentage (%EE) of niosomal tioxlone formulation.

Active ingredient	$\lambda$ max (nm)	Absorbance	Concentration( $\mu$ g/ml)	AmountDialysate (solution)	Total( $\mu$ g/ml)	%EE
Tioxolone	287.9	0.0869	0.0636	85.6	2,000	95.72

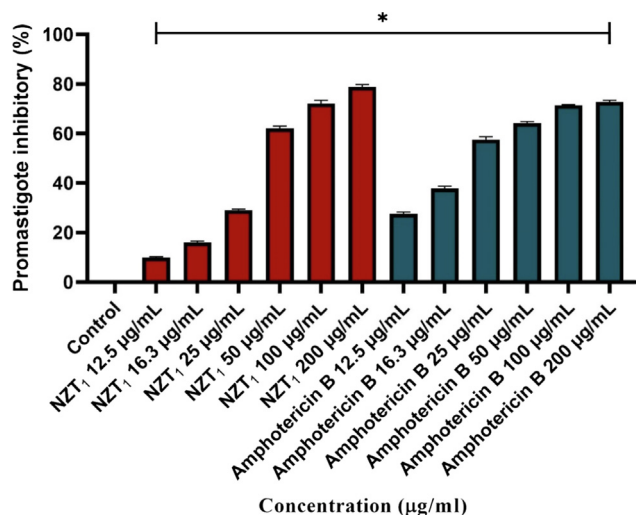


**Fig. 2** The inhibitory rates of *L. major* promastigotes treated with various concentrations of Zr/tioxolone niosomes and amphotericin B after 72 h incubation in comparison with untreated control. Bars represent the mean  $\pm$  SD of inhibitory rates. \* There are significant differences with control group (P-value < 0.0001).

### 3.2. Anti-leishmanicidal effects on promastigotes

The inhibitory rates of *L. major* promastigotes treated with various concentrations of NZTs and the conventional form of amphotericin B demonstrated a dose-dependent pattern, as shown in Fig. 2. The mean inhibition rates of promastigotes treated with various concentrations of NZTs (12.5, 16.3, 25, 50, 100, and 200  $\mu$ g/mL) were 9.65, 15.62, 28.69, 61.52, 71.24, and 78.25, respectively. Moreover, the IC<sub>50</sub> values of NZTs and amphotericin B were  $84.19 \pm 2.38$  and  $41.78 \pm 1.99$   $\mu$ g/mL, respectively. NZTs inhibited the growth of

promastigotes effectively; however, amphotericin B showed a significantly higher inhibitory effect in comparison with the prepared niosomes ( $P < 0.001$ ).

### 3.3. Anti-leishmanicidal effects on intracellular amastigotes

To assess the anti-leishmanicidal activity of amphotericin B and the most effective combination of the niosomal formulation of Zr/tioxolone (NZT<sub>1</sub>) against intracellular amastigotes, the average number of amastigotes in 100 macrophages at various concentrations of drugs was evaluated. According to the results presented in Table 4, the number of intra-macrophage amastigotes was significantly reduced except at the concentration of 12.5  $\mu$ g/mL NZT<sub>1</sub> in comparison with the untreated control. In addition, since the IC<sub>50</sub> values of NZT<sub>1</sub> and amphotericin B against the intra-macrophage parasites were calculated to be  $126.33 \pm 17.07$  and  $28.01 \pm 4.30$ , respectively, amphotericin B was found to be more effective than the niosomal formulation of Zr/tioxolone. However, in the niosomal formulation of Zr/tioxolone, by increasing the concentration, the number of amastigotes was decreased; therefore, it can be concluded that the inhibitory rates of intra-macrophage parasites exhibited a dose-dependent pattern.

### 3.4. Toxicity assay

To determine the cytotoxicity of the drugs, various concentrations of amphotericin B and NZT<sub>1</sub> (25–100  $\mu$ g/mL) were administered to the macrophage cell line. The CC<sub>50</sub> of each drug was assessed based on the level of apoptosis. According to the cytotoxicity analysis, the viability rates of macrophages after the treatment showed a significant difference in comparison with the untreated control ( $P < 0.0001$ ) as indicated in Fig. 3. In addition, increasing the concentration of each drug led to the reduction of the viability rate of macrophages. The viability rates of macrophages at the concentrations of 25, 50, and 100  $\mu$ g/mL NZTs were 84.70, 80.15, and 75.10, respectively, in comparison with the untreated cells (98.40 %). The

**Table 4** Comparison of the overall mean effect of various concentrations of Zr/tioxolone niosome and amphotericin B on the mean number of amastigotes in each macrophage.

Concentrations ( $\mu$ g/mL)	Zr/tioxolone niosome		Amp B	
	Mean $\pm$ SD	P value	Mean $\pm$ SD	P value
0 (Control)	52 $\pm$ 0.62	NR	52 $\pm$ 0.62	NR
12.5	46 $\pm$ 0.17	ns	31 $\pm$ 0.82	$P < 0.001$
16.3	43 $\pm$ 0.77	$P < 0.05$	31 $\pm$ 0.30	$P < 0.001$
25	42 $\pm$ 0.26	$P < 0.05$	30 $\pm$ 0.58	$P < 0.001$
50	36 $\pm$ 0.63	$P < 0.001$	25 $\pm$ 0.37	$P < 0.001$
100	27 $\pm$ 0.75	$P < 0.001$	19 $\pm$ 0.11	$P < 0.001$
200	24 $\pm$ 0.98	$P < 0.001$	16 $\pm$ 0.65	$P < 0.001$

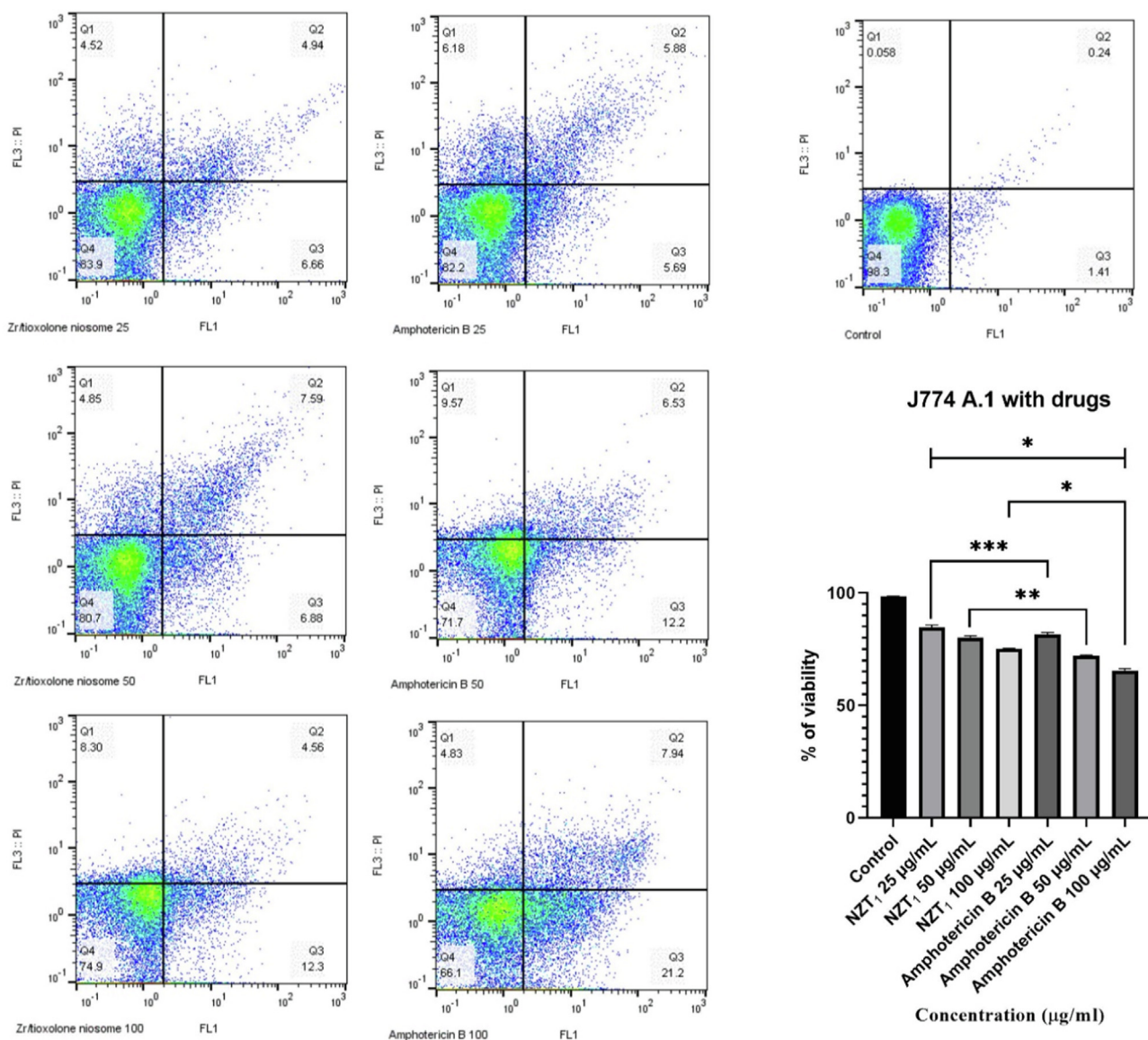


**Fig. 3** The apoptotic and necrotic and viability profiles of J774 A.1 cells in the presence of various concentrations of Zr/tioxolone niosomes and amphotericin B as positive control in comparison with untreated control after 72 h incubation. Bars represent the mean  $\pm$  standard deviation of viability rates (\* $P < 0.0001$ , \*\* $P < 0.001$ , \*\*\* $P < 0.05$ ). There are significant differences with control group ( $P < 0.0001$ ).

$CC_{50}$  of NZTs and amphotericin B was 308.21 and 175.77  $\mu\text{g}/\text{mL}$ , respectively. The results revealed that the mean number of viable cells following treatment with amphotericin B was more than the NZT treatment at similar concentrations.

The selectivity index (SI) was considered to evaluate the cytotoxicity of the treatment in macrophages. As shown in Table 5, the SI for amphotericin B and NZT<sub>1</sub> was calculated to be 6.28 and 2.44, respectively. Therefore, the inhibitory effects of amphotericin B were significantly higher than those of the prepared niosomes due to their SI.

### 3.5. Parasitic apoptosis

In order to evaluate the levels of apoptotic, necrotic, and viable cells at different concentrations of NZT<sub>1</sub>, Annexin V-

FITC and 7-AAD were simultaneously used. For this purpose, the sum of the upper right (late apoptosis) [Annexin V (+), 7-AAD (+)] and lower right regions (early apoptosis) [Annexin V (+), 7-AAD (-)] was calculated and considered as apoptotic cells (Fig. 4). According to the flow cytometry analysis, the apoptotic values at various NZT<sub>1</sub> concentrations (25, 50, 100, and 200  $\mu\text{g}/\text{mL}$ ) were 47.20, 52.50, 54.80, and 65.70, respectively. Various concentrations of the prepared niosomes led to a relatively high rate of apoptosis compared to the untreated control group ( $P < 0.0001$ ).

### 3.6. Antioxidant activity

In order to evaluate the radical-scavenging activity of the niosomal form of Zr/tioxolone (NZT) and BHA (positive control)

**Table 5** Comparison of the  $IC_{50}$  values of amphotericin B and most effective combination of niosomal formulation of Zr/tioxolone (NZT<sub>1</sub>) on the *L. major* promastigotes and amastigotes and the  $CC_{50}$  values of the drugs on macrophage using the SI index.

Drugs	Amastigote $IC_{50}$ ( $\mu\text{g/ml}$ )	Promastigote $IC_{50}$ ( $\mu\text{g/ml}$ )	Macrophage $CC_{50}$ ( $\mu\text{g/ml}$ )	selectivity index $CC_{50}/IC_{50}$ (amastigote)
NZT <sub>1</sub>	126.33	84.19	308.21	2.44
Amp B	28.01	41.78	175.77	6.28

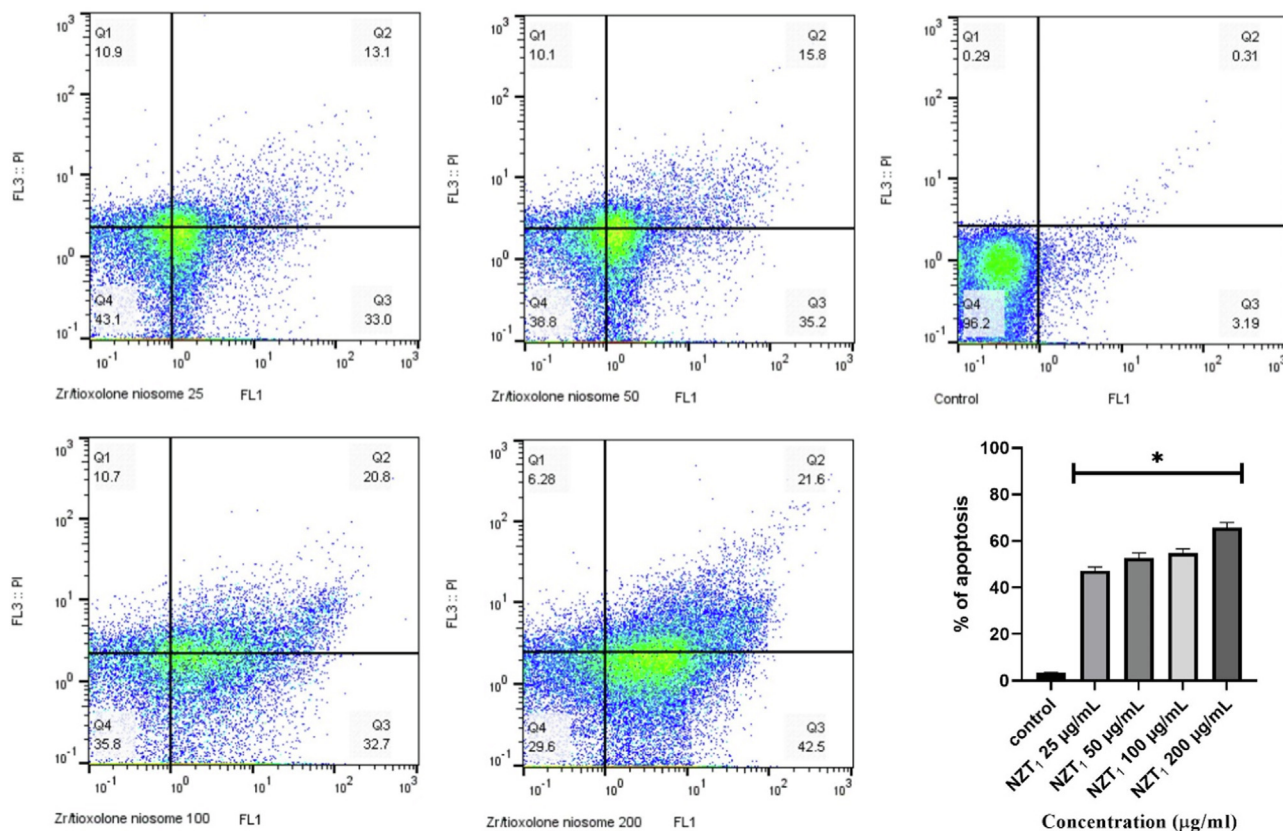


**Fig. 4** The inhibitory rates of *L. major* promastigotes treated with various concentrations of Zr/tioxolone niosomes in comparison with untreated control after 72 h incubation. Bars represent the mean  $\pm$  standard deviation of viability rates. \*There are significant differences with control group ( $P < 0.0001$ ).

against DPPH, the hydrogen donations from these compounds were assessed. As shown in Fig. 5, both BHA and NZT had dose-dependent responses. The overall  $IC_{50}$  values of the prepared niosomes and BHA were 569.1 and 164.9  $\mu\text{g/ml}$ , respectively. According to the statistical analysis, a significant difference was observed between BHA and NZT, although NZT had a relatively high rate of radical-scavenging activity compared to the untreated control group ( $P < 0.001$ ).

### 3.7. ROS detection

The intracellular level of ROS in intra-macrophage amastigotes in response to various concentrations of NZT<sub>1</sub> and amphotericin B was assessed using a fluorescence microscope (Fig. 6). According to the representative images, the production rate of ROS had a dose-dependent pattern. The results

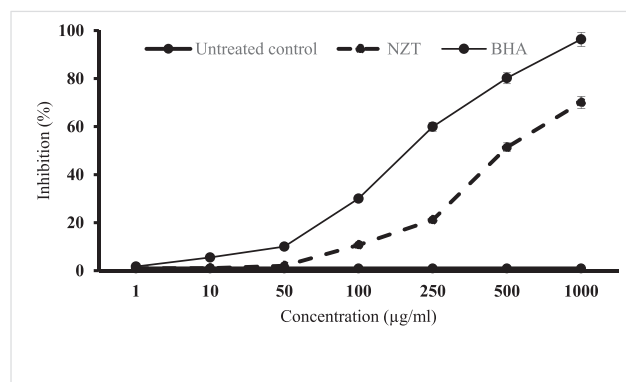


**Fig. 5** Scavenging effects of niosomal form of Zr/tioxolone (NZT) on DPPH free radicals compared to BHA as a positive control. Data are mean  $\pm$  SD of triplicate experiments.

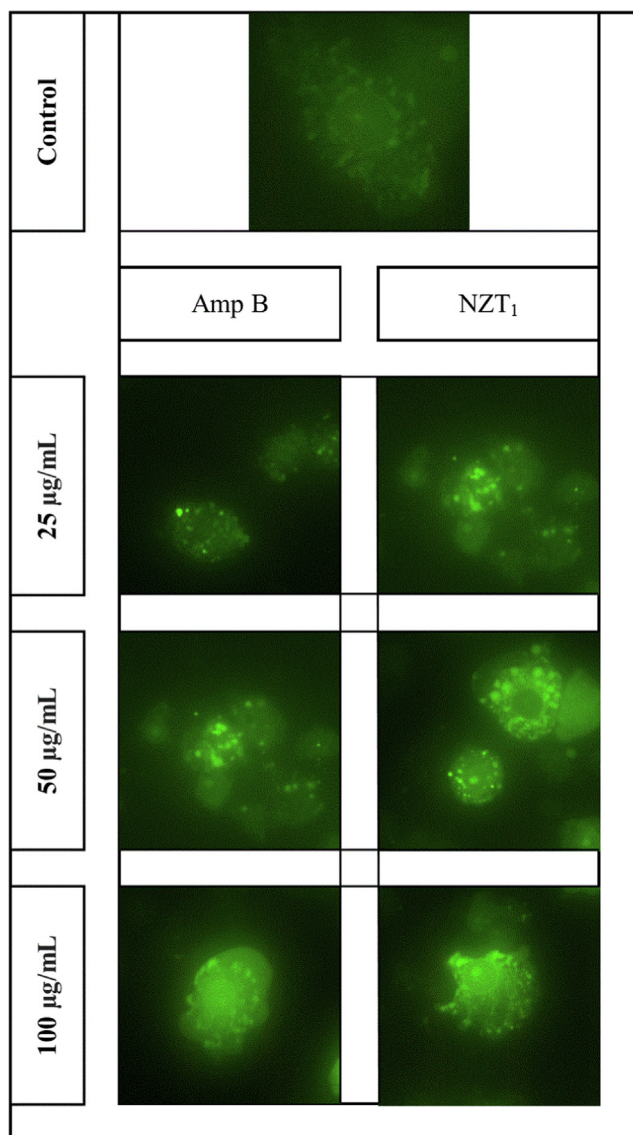


**Fig. 6** In vitro detection of ROS in intra-macrophage amastigotes of *L. major* in response to various concentrations (25, 50 and 100 µg/mL) of amphotericin B and NZT<sub>1</sub> in comparison with untreated control after 72 h incubation.

demonstrated that both NZT<sub>1</sub> and amphotericin B increase the levels of ROS in intra-macrophage amastigotes. The outcomes revealed higher ROS levels in response to NZT<sub>1</sub> in comparison with amphotericin B at similar concentrations.

### 3.8. SOD enzyme activity and nitrite assay

As shown in Fig. 7a, the results were expressed as a unit of SOD, which was defined as the amount of enzyme required to demonstrate 50 % dismutation of the superoxide radicals. Although a significant increase was observed in SOD activity in treated samples compared to untreated control ( $P < 0.001$ ), no significant difference was found between NZT<sub>1</sub> and amphotericin B at the concentration of 100 µg/mL. Fig. 7b depicts nitrite concentrations in axenic amastigotes estimated by a comparison with a standard curve pre-

pared with sodium nitrite. In comparison with the untreated control, higher levels of nitrite were observed, especially at 50 and 100 µg/mL ( $*P < 0.001$ ,  $**P < 0.01$ ). Nearly similar levels of nitrite were reached in samples treated with high concentrations of NZT<sub>1</sub> and amphotericin B.

### 3.9. Gene expression

As representatives of the Th1 and Th2 pathways, the gene expression levels of IL-12 p40 and IL-10 were evaluated. These gene expression levels were assessed against various concentrations of NZT<sub>1</sub> and amphotericin B. As shown in Fig. 8, the gene expression levels of IL-12 p40 and iNOS were significantly up-regulated. The gene expression level of IL-10 was significantly decreased at NZT<sub>1</sub> concentrations of 25 to 100 µg/mL compared to the untreated control ( $P < 0.0001$ ), whilst its expression level at high concentrations (50 and 100 µg/mL) of amphotericin B was only significantly different from the untreated control. Moreover, the results showed a significantly elevated expression of iNOS at various concentrations of both NZT<sub>1</sub> and amphotericin B.

## 4. Discussion

Conventional anti-leishmanial regimens such as pentavalent antimonials and amphotericin B are used in the first-line systemic treatment of leishmaniasis. Due to disadvantages including side effects, low efficacy, parasite resistance, high price, and interactions with other medications, newer chemotherapeutic agents and vesicular drug delivery systems such as niosomes need to be introduced (Yasinzai et al., 2013; Mosimann et al., 2018). Topical treatment of *Leishmania* amastigotes that live in macrophages in the deep dermal layer is one of the difficulties of current chemotherapy (Owais and Gupta, 2005). The best strategy to overcome this drug resistance, reduce the length of treatment, and increase the efficacy rate against CL is combination therapy with novel compounds. In addition, the application of controlled and targeted drug delivery systems such as niosomes and liposomes is considered to be an effective approach (Lobanov et al., 2006; Uchegbu and Florence, 1995). Hence, in this study, the anti-leishmanial activity of the niosomal combination of zirconium and tioxolone against *L. major* was assessed. According to physicochemical properties such as morphology, particle size, physical stability, and entrapment efficiency of the prepared niosomes, the best formulation was chosen as Span/Tween 40 (NZT<sub>1</sub>). Since using niosomes as a novel system for delivering drugs through the skin to the site of infection can reduce the cytotoxicity of drugs, the SI was considered in order to evaluate the cytotoxicity of the niosomes in macrophages (Khazaeli et al., 2014). According to the IC<sub>50</sub> values for the DPPH method (IC<sub>50</sub> of 569.1 µg/mL), NZTs were able to decrease the stable free radical DPPH. This mechanism of action can be suppressed in the occurrence of cell degeneration, cancer, and other diseases, reducing the toxicity of the drug (Sharifi et al., 2018). Based on the results, niosomal formulations of Zr/tioxolone demonstrated no cytotoxic effect within the range of our experimental concentrations because of their target delivery of drugs ( $CC_{50} > 300$  µg/mL and  $SI > 1$ ) (Neira et al., 2019). In this study, due to the higher IC<sub>50</sub> value of the prepared niosomes acting on the promastig-

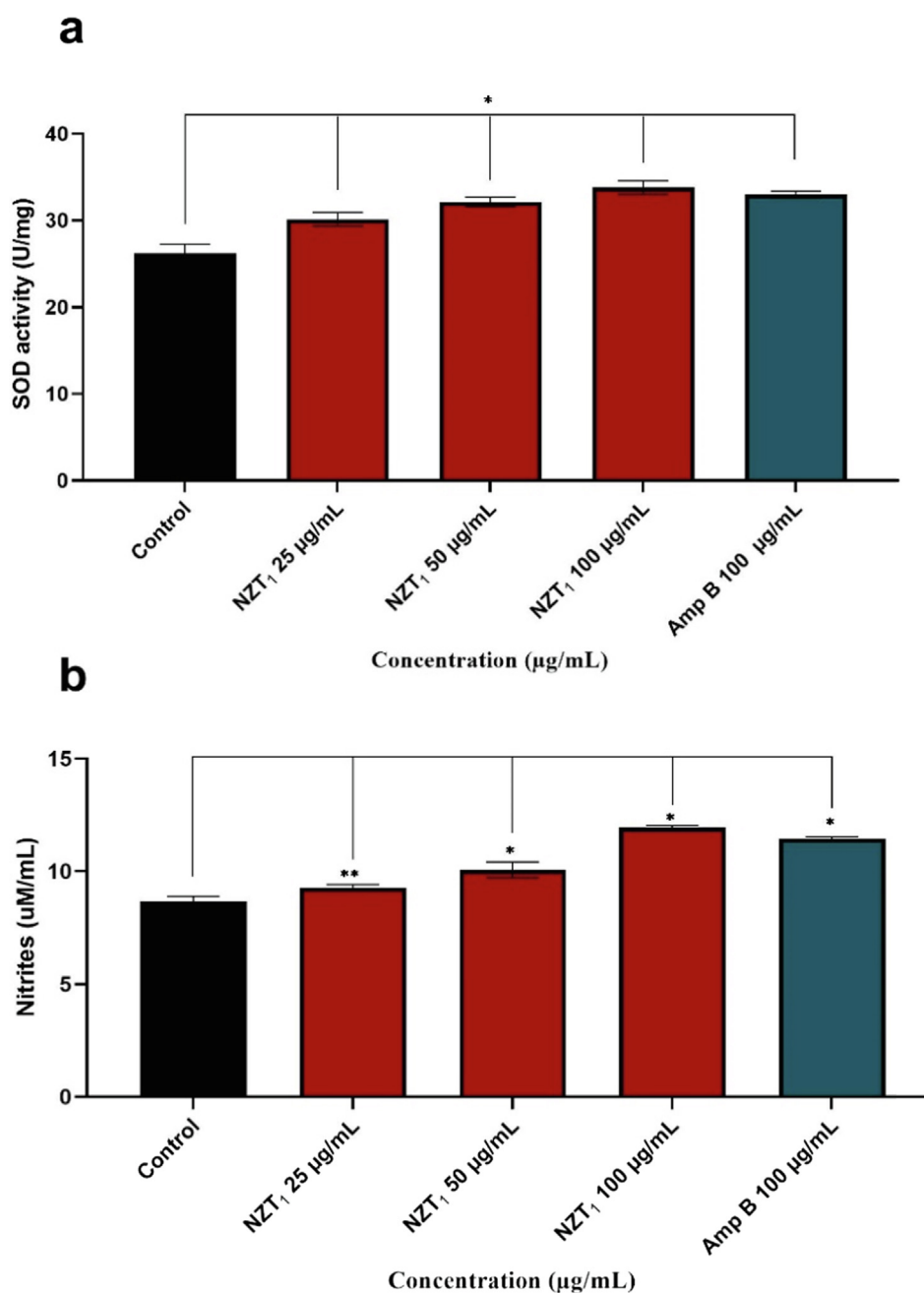


**Fig. 7** (a) Superoxide Dismutase Activity Assay of Samples and untreated control using SOD assay kit. (b) level of nitrite concentrations in axenic amastigotes treated with of niosomal formulation of Zr/tioxolone (NZT<sub>1</sub>) and amphotericin B comparing with untreated control. data represents mean  $\pm$  SD of triplicate determinations. There are significant differences with control group (\* $P < 0.001$ , \*\* $P < 0.01$ ).

ote form of *L. major* compared to the  $IC_{50}$  value of those acting on the amastigote form, it can be concluded that promastigotes were more sensitive to niosomes than the amastigote forms. Several factors can be effective in explaining this difference in sensitivity between the two forms of *L. major*, including the phagolysosomal membrane of macrophages and the prevention of NZTs entrance (Shakibaie et al., 2010; Beheshti et al., 2013). Different biochemical and physiological reactions of these two forms of Leishmania parasites and other

factors such as structural and morphological features can also explain this difference (Lira et al., 1999; Mahmoudvand et al., 2014). In the present study, apoptosis as the programmed cell death of *L. major* promastigotes treated with various concentrations of the prepared niosomes was assessed and the results showed a relatively high rate of apoptosis compared to the untreated control group ( $P < 0.0001$ ).

Leishmania infection can activate two different immune responses including Th1, which is an immune response against

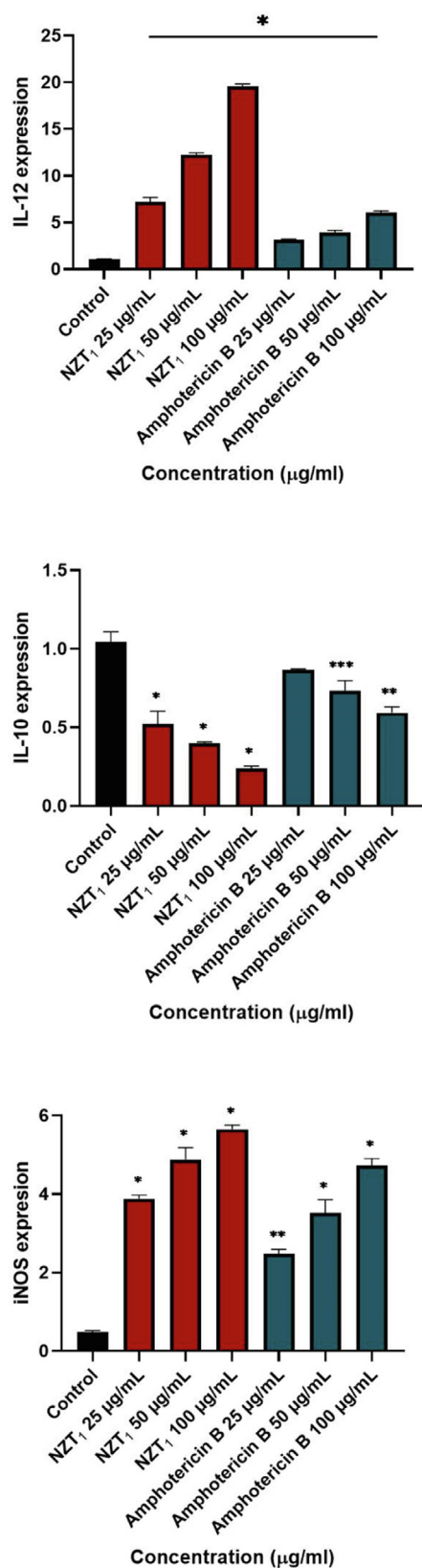


**Fig. 8** The gene expression profiles of IL-12, IL-10 and iNOS in various concentrations of most effective combination of niosomal formulation of Zr/tioxolone (NZT<sub>1</sub>) and amphotericin B in comparison with untreated control; (\* $P < 0.0001$ , \*\* $P < 0.001$ , \*\*\* $P < 0.01$ ).

the *Leishmania* infection (interferon- $\alpha$ , tumor necrosis factor- $\alpha$ , IL-12, and NO) and Th2, which can contribute to the disease progression (IL-4, IL-10, IL-13, and transforming growth factor- $\beta$ ) (Mostafavi et al., 2019; Prajapati et al., 2011). Th1-type immunity can be activated by the expression of cytokines, namely interferon- $\alpha$ , tumor necrosis factor- $\alpha$ , and IL-12, and consequently activate macrophages to generate NO. In contrast, IL-10 plays a crucial role in activating Th2-type cell response and suppression of macrophage activation [46–48]. According to our findings, NZTs had a significant immunomodulatory effect on the inhibition of IL-10 as an indicator of Th2-type immunity compared to the untreated control ( $P < 0.0001$ ). In addition, the results revealed a significant increase in the gene expression level of IL-12 and iNOS as markers of Th1-type immunity ( $P < 0.0001$ ).

ROS generation can lead to the decreased survival of the *Leishmania* parasite by increasing lipid peroxidation and activating apoptosis [49–51]. Adjustment of cellular growth and cell death can be affected by superoxide and hydrogen peroxide ( $H_2O_2$ ) as different forms of ROS (Circu et al., 2010). Upregulation of the antioxidant defense is one of the defense mechanisms of the parasite to control the level of ROS in order to protect itself from ROS-mediated apoptosis (Ha et al., 1998; Fujisawa and Kadoma, 2005). SOD is one of the defense mitochondrial enzymes that can detoxify superoxide into hydrogen peroxide and oxygen and consequently protect the parasites from mitochondrial-derived ROS damage, oxidative stress, and apoptosis (Pleues et al., 2003; Getachew et al., 2012). Our findings indicated higher ROS levels in NZT<sub>1</sub> treatment in comparison with amphotericin B treatment at similar concentrations in a dose-dependent response. In addition, a significant increase in SOD activity was observed in treated samples compared to untreated controls ( $P < 0.001$ ), and no significant difference was found between NZT<sub>1</sub> and amphotericin B at the concentration of 100 µg/mL. Overexpression of SOD in *L. major* parasites indicated an enhanced protection due to the higher generation of free radical agents by macrophages (Bahrami et al., 2011). NZTs could increase NO production, which is crucial for controlling *Leishmania major* propagation or eliminating the parasite (Elmahallawy et al., 2014). However, nitrite levels were non-significantly higher in samples treated with NZT<sub>1</sub> than in those treated with amphotericin B at a similar concentration.

## 5. Conclusion

According to the literature, the present study is the first to investigate the anti-leishmanial activity of zirconium plus tioxolone niosomes against *Leishmania major* by evaluating their mechanism of action. In addition, the results revealed an immunomodulatory role in the inhibition of IL-10 and an increase in gene expression levels of IL-12 and iNOS. The present findings indicated that NZT<sub>1</sub> had the potential for further therapeutic approaches due to its beneficial physicochemical properties and strong anti-leishmaniasis effects against *L. major* after further assessments including comprehensive clinical trials.

## Declaration of Competing Interest

The authors declare that they have no known competing financial interests or personal relationships that could have appeared to influence the work reported in this paper.

## Acknowledgments

Authors are grateful to council of Pharmaceutics Research Center, Institute of Neuropharmacology, Local ethical and tracking code 99000621 received from the Kerman University of Medical Sciences for this study.

## References

- Akbari, M., Oryan, A., Hatam, G., 2017. Application of nanotechnology in treatment of leishmaniasis: a review. *Acta tropica* 172, 86–90.
- Bahrami, S., Hatam, G., Razavi, M., Nazifi, S., 2011. In vitro cultivation of axenic amastigotes and the comparison of antioxidant enzymes at different stages of *Leishmania tropica*. *Trop Biomed.* 28 (2), 411–417.
- Bahraminegad, S., Pardakhty, A., Sharifi, I., Ranjbar, M., 2021. Therapeutic effects of the as-synthesized polylactic acid/chitosan nanofibers decorated with amphotericin B for in vitro treatment of leishmaniasis. *J. Saudi Chem. Soc.*
- Bahraminegad, S., Pardakhty, A., Sharifi, I., Ranjbar, M., 2021. The assessment of apoptosis, toxicity effects and anti-leishmanial study of Chitosan/CdO core-shell nanoparticles, eco-friendly synthesis and evaluation. *Arab. J. Chem.* 14 (4), 103085.
- Baillie, A., Coombs, G., Dolan, T., Laurie, J., 1986. Non-ionic surfactant vesicles, niosomes, as a delivery system for the anti-leishmanial drug, sodium stibogluconate. *J. Pharm. Pharmacol.* 38 (7), 502–505.
- Beheshti, N., Soflaei, S., Shakibaie, M., Yazdi, M.H., Ghaffarifar, F., Dalimi, A., Shahverdi, A.R., 2013. Efficacy of biogenic selenium nanoparticles against *Leishmania major*: in vitro and in vivo studies. *J. Trace Elements Med. Biol.* 27 (3), 203–207.
- Bogdan, C., Vodovotz, Y., Nathan, C., 1991. Macrophage deactivation by interleukin 10. *J. Exp. Med.* 174 (6), 1549–1555.
- Bucks, D., Sarpotdar, P., Yu, K., Angel, A., Del Rosso, J., 2009. The development and optimization of a fixed combination of clindamycin and benzoyl peroxide aqueous gel. *J. Drugs Dermatol.: JDD* 8 (7), 634–638.
- Chandra, D., Naik, S., 2008. *Leishmania donovani* infection down-regulates TLR2-stimulated IL-12p40 and activates IL-10 in cells of macrophage/monocytic lineage by modulating MAPK pathways through a contact-dependent mechanism. *Clin. Exp. Immunol.* 154 (2), 224–234.
- Circu, M.L., Aw, T.Y., 2010. Reactive oxygen species, cellular redox systems, and apoptosis. *Free Rad. Boil. Med.* 48 (6), 749–762.
- de Carvalho, R.F., Ribeiro, I.F., Miranda-Vilela Filho, A.L., de Souza, J., Martins, O.P., e Silva, D.D., Tedesco, A.C., Lacava, Z. G., Bão, S.N., Sampaio, R.N., 2013. Leishmanicidal activity of amphotericin B encapsulated in PLGA–DMSA nanoparticles to treat cutaneous leishmaniasis in C57BL/6 mice. *Exp. Parasitol.* 135 (2), 217–222.
- Elmahallawy, E.K., Jiménez-Aranda, A., Martínez, A.S., Rodríguez-Granger, J., Navarro-Alarcón, M., Gutiérrez-Fernández, J., Agil, A., 2014. Activity of melatonin against *Leishmania infantum* promastigotes by mitochondrial dependent pathway. *Chemico-biol. Interact.* 220, 84–93.
- Fujisawa, S., Kadoma, Y., 2005. Kinetic evaluation of polyamines as radical scavengers. *Anticancer Res.* 25 (2A), 965–969.
- Gannavaram, S., Bhattacharya, P., Ismail, N., Kaul, A., Singh, R., Nakhasi, H.L., 2016. Modulation of innate immune mechanisms to enhance *Leishmania* vaccine-induced immunity: role of coinhibitory molecules. *Front. Immunol.* 7, 187.
- Getachew, F., Gedamu, L., 2012. *Leishmania donovani* mitochondrial iron superoxide dismutase A is released into the cytosol during miltefosine induced programmed cell death. *Mole. Biochem. Parasitol.* 183 (1), 42–51.
- Ha, H.C., Sirisoma, N.S., Kuppusamy, P., Zweier, J.L., Woster, P.M., Casero Jr, R.A., 1998. The natural polyamine spermine functions directly as a free radical scavenger. *Proc. Natl. Acad. Sci.* 95 (19), 11140–11145.
- Hu, C., Rhodes, D.G., 1999. Proniosomes: a novel drug carrier preparation. *Int. J. Pharmac.* 185 (1), 23–35.
- Hunter, C.A., Dolan, T.F., Coombs, G.H., Baillie, A.J., 1988. Vesicular systems (niosomes and liposomes) for delivery of sodium stibogluconate in experimental murine visceral leishmaniasis. *J. Pharm. Pharmacol.* 40 (3), 161–165.
- Irigoin, F., Inada, N.M., Fernandes, M.P., Piacenza, L., Gadelha, F. R., Vercesi, A.E., Radi, R., 2009. Mitochondrial calcium overload triggers complement-dependent superoxide-mediated programmed cell death in *Trypanosoma cruzi*. *Biochem. J.* 418 (3), 595–604.
- Jain, N.K., 1997. *Controlled and Novel Drug Delivery*. CBS Publishers & Distributors.
- Kazi, K.M., Mandal, A.S., Biswas, N., Guha, A., Chatterjee, S., Behera, M., Kuotsu, K., 2010. Niosome: a future of targeted drug delivery systems. *J. Adv. Pharmac. Technol. Res.* 1 (4), 374.
- Khazaeli, P., Sharifi, I., Talebian, E., Heravi, G., Moazeni, E., Mostafavi, M., 2014. Anti-leishmanial effect of itraconazole niosome on in vitro susceptibility of *Leishmania tropica*. *Environ. Toxicol. Pharmacol.* 38 (1), 205–211.
- Koutsoni, O., Barhoumi, M., Guizani, I., Dotsika, E., 2014. *Leishmania* eukaryotic initiation factor (LeIF) inhibits parasite growth in murine macrophages. *PLoS One* 9 (5).
- Kumari, D., Perveen, S., Sharma, R., Singh, K., 2021. Advancement in leishmaniasis diagnosis and therapeutics: an update. *Eur. J. Pharmacol.* 910.
- Lira, R., Sundar, S., Makharia, A., Kenney, R., Gam, A., Saraiva, E., Sacks, D., 1999. Evidence that the high incidence of treatment failures in Indian kala-azar is due to the emergence of antimony-resistant strains of *Leishmania donovani*. *J. Infect. Dis.* 180 (2), 564–567.
- Lobanov, A.V., Gromer, S., Salinas, G., Gladyshev, V.N., 2006. Selenium metabolism in *Trypanosoma*: characterization of selenoproteomes and identification of a Kinetoplastida-specific selenoprotein. *Nucl. Acids Res.* 34 (14), 4012–4024.
- Mahmoudvand, H., Shakibaie, M., Tavakoli, R., Jahanbakhsh, S., Sharifi, I., 2014. In vitro study of leishmanicidal activity of biogenic selenium nanoparticles against Iranian isolate of sensitive and glucantime-resistant *Leishmania tropica*. *Iran. J. Parasitol.* 9 (4), 452.
- Mandal, A., Das, S., Roy, S., Ghosh, A.K., Sardar, A.H., Verma, S., Saini, S., Singh, R., Abhishek, K., Kumar, A., Mandal, C., 2016. Deprivation of L-arginine induces oxidative stress mediated apoptosis in *Leishmania donovani* promastigotes: contribution of the polyamine pathway. *PLoS Negl. Trop. Dis.* 10 (1).
- Medda, S., Mukhopadhyay, S., Basu, M.K., 1999. Evaluation of the in-vivo activity and toxicity of amarogentin, an antileishmanial agent, in both liposomal and niosomal forms. *J. Antimicrob. Chemother.* 44 (6), 791–794.
- Miret, J.A., Moreno, J., Nieto, J., Carter, K.C., Mullen, A.B., Ambros, L., Rodríguez, C., San Andrés, M.I., González, F., 2021. Antileishmanial efficacy and tolerability of combined treatment with non-ionic surfactant vesicle formulations of sodium stibogluconate and paromomycin in dogs. *Exp. Parasitol.* 220.
- Miret, J.A., Moreno, J., Nieto, J., Carter, K.C., Mullen, A.B., Ambros, L., Rodríguez, C., San Andrés, M.I., González, F., 2016. Antileishmanial efficacy and tolerability of combined treatment with non-ionic surfactant vesicle formulations of sodium stibogluconate and paromomycin in dogs. *Exp. Parasitol.* 220.
- Monzote, L., 2009. Current treatment of leishmaniasis: a review. *Open Antimicrob. Agents J.* 1 (1).
- Mosimann, V., Neumayr, A., Paris, D.H., Blum, J., 2018. Liposomal amphotericin B treatment of Old World cutaneous and mucosal leishmaniasis: a literature review. *Acta Tropica* 182, 246–250.

- Mostafavi, M., Farajzadeh, S., Sharifi, I., Khazaeli, P., Sharifi, H., 2019. Leishmanicidal effects of amphotericin B in combination with selenium loaded on niosome against *Leishmania tropica*. *J. Parasitic Dis.* 43 (2), 176–185.
- Mostafavi, M., Khazaeli, P., Sharifi, I., Farajzadeh, S., Sharifi, H., Keyhani, A., Parizi, M.H., Kakooei, S., 2019. A novel niosomal combination of selenium coupled with glucantime against *Leishmania tropica*. *Korean J. Parasitol.* 57 (1), 1.
- Müller, R.H., Jacobs, C., Kayser, O., 2001. Nanosuspensions as particulate drug formulations in therapy: rationale for development and what we can expect for the future. *Adv. Drug Deliv. Rev.* 47, 3–19.
- Neira, L.F., Mantilla, J.C., Escobar, P., 2019. Anti-leishmanial activity of a topical miltefosine gel in experimental models of New World cutaneous leishmaniasis. *J. Antimicrob. Chemother.* 74 (6), 1634–1641.
- W.H. Organization, 2017. Integrating Neglected Tropical Diseases into Global Health and Development: Fourth WHO Report on Neglected Tropical Diseases. World Health Organization.
- Owais, M., Gupta, C.M., 2005. Targeted drug delivery to macrophages in parasitic infections. *Curr. Drug Deliv.* 2, 311–318.
- Pardakhty, A., Shakibaie, M., Daneshvar, H., Khamesipour, A., Mohammadi-Khorsand, T., Forootanfar, H., 2012. Preparation and evaluation of niosomes containing autoclaved *Leishmania major*: a preliminary study. *J. Microencaps.* 29 (3), 219–224.
- Parizi, M.H., Farajzadeh, S., Sharifi, I., Pardakhty, A., Parizi, M.H., Sharifi, H., Salarkia, E., Hassanzadeh, S., 2019. Antileishmanial activity of niosomal combination forms of tioxolone along with benzoxonium chloride against *Leishmania tropica*. *Korean J. Parasitol.* 57 (4), 359.
- Parizi, M.H., Pardakhty, A., Farajzadeh, S., Parizi, M.H., Sharifi, H., Keyhani, A.R., Mostafavi, M., Bamorovat, M., Ghaffari, D., 2019. Antileishmanial activity and immune modulatory effects of benzoxonium chloride and its entrapped forms in niosome on *Leishmania tropica*. *J. Parasitic Dis. Off. Org. Indian Soc. Parasitol.* 43 (3), 406.
- Patil, N.A., Kandasubramanian, B., 2020. Biological and mechanical enhancement of zirconium dioxide for medical applications. *Ceram. Int.* 46 (4), 4041–4057.
- Plewes, K.A., Barr, S.D., Gedamu, L.J.I., 2003. Iron superoxide dismutases targeted to the glycosomes of *Leishmania chagasi* are important for survival. *Infect. Immun.* 71 (10), 5910–5920.
- Prajapati, V.K., Awasthi, K., Gautam, S., Yadav, T.P., Rai, M., Srivastava, O.N., Sundar, S., 2011. Targeted killing of *Leishmania donovani* in vivo and in vitro with amphotericin B attached to functionalized carbon nanotubes. *J. Antimicrob. Chemother.* 66 (4), 874–879.
- Raina, P., Kaur, S., 2012. Knockdown of LdMCI and Hsp70 by antisense oligonucleotides causes cell-cycle defects and programmed cell death in *Leishmania donovani*. *Mole. Cell. Biochem.* 359 (1), 135–149.
- Ridgley, E.L., Xiong, Z.H., Ruben, L., 1999. Reactive oxygen species activate a Ca<sup>2+</sup>-dependent cell death pathway in the unicellular organism *Trypanosoma brucei brucei*. *Biochem. J.* 340 (1), 33–40.
- Shakibaie, M., Khorramizadeh, M.R., Faramarzi, M.A., Sabzevari, O., Shahverdi, A.R., 2010. Biosynthesis and recovery of selenium nanoparticles and the effects on matrix metalloproteinase-2 expression. *Biotechnol. Appl. Biochem.* 56 (1), 7–15.
- Sharifi, F., Shariffar, F., Sharifi, I., Alijani, H.Q., Khatami, M., 2018. Cytotoxicity, leishmanicidal, and antioxidant activity of biosynthesised zinc sulphide nanoparticles using *Phoenix dactylifera*. *Iet Nanobiotechnol.* 12 (3), 264–269.
- Sharifi, I., Tabatabaie, F., Nikpour, S., Mostafavi, M., Olliaee, R.T., Sharifi, F., Babaei, Z., Jafari, E., Salarkia, E., Shahbazzadeh, D., 2021. The Effect of *Naja naja oxiana* Snake Venom Against *Leishmania tropica* Confirmed by Advanced Assays. *Acta Parasitologica* 66 (2), 475–486.
- Singh, K., Garg, G., Ali, V., 2016. Current therapeutics, their problems and thiol metabolism as potential drug targets in leishmaniasis. *Curr. Drug Metabol.* 17, 897–919.
- Singh, S., Sivakumar, R., 2004. Challenges and new discoveries in the treatment of leishmaniasis. *J. Infect. Chemother.* 10, 307–315.
- Steverding, D., 2017. The history of leishmaniasis. *Parasites Vectors* 10 (1), 1–10.
- Uchegbu, I.F., Florence, A., 1995. Non-ionic surfactant vesicles (niosomes): physical and pharmaceutical chemistry. *Adv. Colloid Interf. Sci.* 58, 1–55.
- Vyas, S.P., Gupta, S., as and Gupta 2006. Optimizing efficacy of amphotericin B through nanomodification. *Int. J. Nanomed.* 1 (4), 417.
- Yaszynski, M., Khan, M., Nadhman, A., Shahnaz, G., 2013. Drug resistance in leishmaniasis: current drug-delivery systems and future perspectives. *Future Med. Chem.* 5, 1877–1888.
- Ye, M., Shi, B., 2018. Zirconia nanoparticles-induced toxic effects in osteoblast-like 3T3-E1 cells. *Nanoscale Res. Lett.* 13 (1), 1–12.
- Zhong, M., Wang, X., Wen, J., Cai, J., Wu, C., Aly, S.M., 2013. Selection of reference genes for quantitative gene expression studies in the house fly (*Musca domestica* L.) using reverse transcription quantitative real-time PCR. *Acta Biochim. Biophys. Sin.* 45 (12), 1069–1073.